HHS Public Access

Author manuscript

Top Magn Reson Imaging. Author manuscript; available in PMC 2017 October 01.

Published in final edited form as:

Top Magn Reson Imaging. 2016 October ; 25(5): 197–204. doi:10.1097/RMR.0000000000000105.

Cellular and Molecular Imaging using Chemical Exchange Saturation Transfer (CEST)

Michael T. McMahon[1,2,*] and **Assaf A. Gilad**[1,2,3]

[1] F.M. Kirby Research Center for Functional Brain Imaging, Kennedy Krieger Institute, Baltimore, Maryland [2] The Russell H. Morgan Department of Radiology and Radiological Sciences, Division of MR Research [3] Cellular Imaging Section and Vascular Biology Program, Institute for Cell Engineering, Johns Hopkins University School of Medicine, Baltimore, Maryland

Abstract

Chemical Exchange Saturation Transfer (CEST) is a powerful new tool well suited for molecular imaging. This technology enables the detection of low concentration probes through selective labeling of rapidly exchanging protons or other spins on the probes. In this review, we will highlight the unique features of CEST imaging technology and describe the different types of CEST agents which are suited for molecular imaging studies including CEST theranostic agents, CEST reporter genes, and CEST environmental sensors.

Keywords

CEST; diaCEST; paraCEST; molecular imaging; contrast agents

1. Introduction

Chemical Exchange Saturation Transfer (CEST) is a powerful new tool well suited for molecular imaging (1-4). This technology enables the detection of low concentration probes through selective labeling of rapidly exchanging protons or other spins on the probes. The transfer of saturation from one molecule to another was first observed in 1963 by Sture Forsén and Ragnar Hoffman (5,6), however it was not so clear that this technique would be applicable to magnetic resonance imaging until Steve Wolff, Robert Balaban and colleagues demonstrated the detection of compounds of interest for medical imaging with exchangeable protons through saturation transfer imaging, urea and ammonia (7,8). As has now been clearly shown, for exchangeable spins at low concentration (nM-mM range) a cumulative effect (Molar range) can be built up and detected provided the spins have a sufficiently high exchange rate (k_{ex}), allowing production of high contrast images (4,9). Fig. 1 demonstrates the basic principles of signal amplification using CEST imaging. As is shown, after applying a saturation pulse, signal contrast can be detected through measuring the asymmetric Magnetization Transfer Ratio (MTR_{asym}) which is the normalized difference in water signal

[*]TELEPHONE: mcmahon@mri.jhu.edu, 443-923-9356.
assaf.gilad@jhu.edu, 410-502-8188

between the two experiments, one with the RF field on resonance with the exchangeable peak and the other with the RF field at the same frequency away from water but on the opposite side (10-14). Based on this mechanism for generating contrast, CEST probes have a few unique features. Because the labile spins resonate over a range of chemical shifts, imaging schemes have been developed to discriminate between agents possessing these spins simultaneously, which has been called multi-color (15-17) or multi-frequency MRI (2,18). This labeling feature makes CEST agents unlike T1 or T2* MRI contrast agents, and instead more similar to optical imaging agents. CEST contrast generally increases as the scanner magnetic field increases, which makes this a favorable approach compared to T1 relaxation agents whose contrast will be reduced at higher fields through T1 relaxation time convergence (19). Because of these features, a large number of groups have focused on developing CEST contrast agents for a variety of cellular and molecular imaging applications.

2. Small molecule CEST probes

A major emphasis in CEST imaging has been placed on development of natural, diamagnetic CEST (diaCEST) agents, as there is an enormous variety, which possesses labile protons. In fact, the first compounds presented as CEST agents suitable for medical imaging were urea and ammonia (7,8). More recent studies have investigated detection of D-glucose (20-22), glutamate (23,24), creatine (24,25), and L-arginine (26) on 7 T and higher field scanners. As a result of the interest in developing agents for detection on 3 T and lower field scanners, recent studies have emphasized the design of compounds with chemical shifts from water ($\Delta\omega$) > 4 ppm (27). Based on this criteria, barbituric acid (28,29), thymidine analogs (30), iodinated compounds (31-33), imidazoles (34) salicylic acid and anthranilic acid analogs have come to the forefront. The salicylates and anthranillates are particularly appealing based on their chemical structure consisting of a phenol proton hydrogen bonded to a carboxylate, which has been known with large chemical shift (35-37) which is particularly favorable for 3 T scanners based on their $\Delta\omega$ = 6 -12 ppm and the capability of tuning k_{ex} from 400 - 3000 s^{-1}, suitable rates for detection of CEST contrast. Fig. 2 shows a range of MTR_{asym} spectra for these probes. The salicylates seem well suited for detection of perfusion (38). Some of the first investigational CEST patient studies have now been performed utilizing the diaCEST agents glucose and iopamidol, with the idea that these agents might present advantages for tumor imaging, with the initial images appearing quite encouraging (39,40).

A second focus for this field is on design CEST probes using paramagnetic metal complexes similar to those used as T1 agents. Sherry (41,42), Aime (43,44), and others (45-52) have pioneered the use of paramagnetic metal based CEST agents with appropriately shifted labile protons, which have been termed as paramagnetic CEST (paraCEST) probes. The labile proton $\Delta\omega$ can be increased to between 30-700 ppm for these systems based on hyperfine shifts allowing detection of protons with larger k_{ex} while still adhering to the slow-intermediate exchange condition (1,53-57). The labile protons can be a whole water molecule coordinated to the metal and exchanging on/off the complex, or they can be amide, amine or alcohol protons on the complex with suitable configurations with respect to the paramagnetic center. To date, paraCEST agents have been only applied in pre-clinical

studies, however these agents represent the most promising for detection on 1 - 1.5 T scanners (58). Indeed, as HPDO3A has already been approved for patient studies as a safe chelator of Gadolinium and is in use in clinical practice (Prohance, Bracco Imaging, Milan, Italy), one could reasonably expect that paraCEST agents based on HPDO3A could be translated for generating pH maps of tumors, which could be useful in monitoring tumor microenvironment (59).

3. CEST probes as theranostic agents

An exciting area, which appears quite promising, is to utilize CEST imaging to monitor the delivery of therapeutics. This is a very active area of research. Based on sensitivity considerations, a majority of the studies have emphasized use of delivery systems with both CEST probe and therapeutic integrated into nanocarriers. The approaches have included: conjugating CEST probes to the surface of nanocarriers (60-63), entrapping CEST probes into the interior of the carriers (15,28,29), or a third approach, entrapping shift agents in the interior of the carriers and using the interior solvent as the CEST probe itself, the so-called lipo-CEST approach (64). A number of studies have shown that delivery of therapeutics to tumors can be detected and quantified using this technology (29,60,65). This has been motivated in large part by the possibility of performing multi-color CEST imaging in vivo without penetration depth limitations (Fig. 3). As is shown, two different therapeutics can be labeled with a different color and monitored independently using this technology. Moreover, it was recently demonstrated that CEST MRI can be used to detect a clinically used DNA alkylating anti-cancer agent directly without the need to conjugate or modify the drug (66). This is extremely important because even the addition of the Lest tag (such as a fluorine group) can significantly change the affinity of the drug to the target or reduce its activity. The future appears quite promising for this new technology as contrast agent chemistry, image acquisition schemes and MRI hardware improve.

4. CEST reporter genes for cellular imaging

After the observation was made that biological macromolecules can be detected using CEST agents (67), an intense effort has been put forth to develop CEST agents which might be expressed by cells, so-called CEST reporter genes. This is a particularly interesting area, as this technology would allow the generation of functional information about cells not normally accessible using MRI scans. Developing of these types of agents poses different challenges from the other agents mentioned earlier to formulate an optimal expressable CEST probe, with a number of studies that are summarized in Table 1. Each study was necessary for developing the next step. While early on it was shown by van Zijl and colleagues that Poly-LLysine (PLL) is a good CEST probe (67), optimization was needed to allow expression of this peptide by mammalian cells. Nevertheless, PLL was the foundation for a decade of development of new peptide-based agents. Another important aspect of this work was the development of screening methods for peptide libraries for formulating the next generation of agents (68,69). Advances in gene synthesis technologies significantly reduced costs and shortened the synthesis time (70), which has now led to an increased ability to express many of these proteins in both live mammalian cells and bacteria (71-74).

The ability to synthesize whole proteins (longer the 50 amino acids) allowed deeper investigation of their biophysical properties (75).

In order to ensure the quality of these reporter genes is sufficient for cellular imaging, it is important to demonstrate reproducibility beyond the first “proof-of-concept” paper. This has been demonstrated for the LRP CEST reporter gene; following the initial study where it was shown that the contrast generated from LRP can be differentiated from controls, its practicality has been repeatedly demonstrated in live rodents and enabled collection of high temporal and spatial resolution images (76,77). Farrar and colleagues have confirmed that LRP can be visualized in live rats after delivery of an oncolytic virus, thus serving as a marker for treatment efficacy (78) (Fig. 4). In a separate study, Pomper and colleagues have demonstrated tumor-specific expression of LRP using a tumor-specific promoter (79) (Fig. 5). Interestingly, the PEG3 promoter is weaker than CMV and yet still provided a detectable CEST contrast. These two studies have presented new evidence that LRP is effective for detecting cells through gene expression. Moreover, these studies established the reproducibility of LRP as a reporter gene for MRI.

5. CEST environmental sensors for cellular imaging

While reporter genes such as LRP can be used to monitor cell survival and are well established in a pre-clinical setting, there are challenges to using reporter genes in patients based on the requirement of genetic manipulation of the cells for transplantation. Because of this, we have developed an alternative strategy, which instead employs implantable environmental sensors to monitor rejection of these cell grafts. These sensors are integrated into cell composites. This is a flexible method, as there are a range of MRI probes which have been developed for detecting changes in environment including the pH (32,33,69,80,81) or the concentration of inorganic ions such as Zn^{2+} or Ca^{2+} (50,82-85). Our initial idea was that one effective way to use these sensors would be to embed these in cell composites and monitor the environment post-transplantation. There are three components of these composites: the CEST sensors, the liposomes which entrap the sensors but are sufficiently permeable to water and the hydrogels which provide support for the cell graft (86) (Figure 6). This design isolates the sensor from the cells and also from the immune system while allowing free access of water and ions. One type of environmental change that can be sensed readily using CEST imaging is pH, which influences k_{ex} through acid and base catalysis of proton exchange, with pH changes also linked to cell death (87). Previous hydrogel based cellular MRI studies were concerned with visualizing their location (88,89), so our cell composites with arginine based CEST pH sensors added a new dimension. Our first investigation involved transplanting human hepatocytes subcutaneously within alginate composites, and in order to test the capabilities of these sensors, groups of mice with and without immunosuppression treatment were included with the expectation that cell survival would be prolonged in the immunosuppressed group (90). The hepatocytes were transfected with luciferase to allow usage of bioluminescence to monitor hepatocyte viability for validation. As expected, as the encapsulated cells died, there was a corresponding 33% drop in CEST MRI contrast detected, with also a substantial difference in hepatocyte survival for the immunosuppressed mice compared to the non-immunosuppressed mice, which corresponds to lowering the pH from 7.4 to 6.9. This work was followed up by a separate

investigation of the host immune response to these cell composites, which depended on whether the highly immunogenic HepG2 hepatocytes were included within these composites (91). A higher immune cell infiltration was detected when live hepatocytes were included in the composite (compared to dead hepatocytes), which was presumably associated with xenogeneic molecules passing through the capsule surface. The amount of immune cells surrounding the composites containing hepatocytes was comparable to composites without hepatocytes when FK506 immunosuppression was administered. Based on these studies, we concluded that CEST imaging of cell composites should represent a promising technology for monitoring the functionality of cells after transplantation.

6. Hyperpolarized CEST (hyperCEST) imaging

An alternative strategy to increase the sensitivity of CEST imaging further, is to move away from detecting exchange with water to detecting exchange of hyperpolarized ^{129}Xe, which has been termed hyper-CEST imaging. This strategy was initially reported by Leif Schroeder, Alex Pines and co-workers, and involved use of specialized cage structures which transiently trap and impart a chemical shift on hyperpolarized ^{129}Xe compared to gas phase, with rapid exchange of Xe occurring between the interior and exterior of the cage (92). For molecular imaging studies, ^{129}Xe appears to be the most promising of the noble gases which can be hyperpolarized based on solubility in aqueous solutions (93) and biological tissue (94,95), relative abundance of xenon gas, and also responsiveness of the ^{129}Xe chemical shift to molecular environment. Furthermore, hyperpolarizers have been designed to produce large quantities of polarized Xe-129 gas allowing clinical usage (96-99). This strategy of hyperCEST imaging envisions targeted imaging of these cages after inhalation of xenon gas by patients. Cages have been developed which are sensitized to lead, zinc, mercury and cadmium ions (100-102), which assemble onto a multivalent M13 bacteriophage (103), and report on cellular internalization (104). One particularly nice study showed that bioengineered bacterial gas vesicles enabling detection of picomolar concentrations of the gas-binding protein nanostructures expressed (105). Another interesting study showed that bacterial spores represent another nanoporous structure which can be detected using hyperCEST imaging (106). This strategy, which involves hyperpolarized Xenon with the polarization dropping with T1, has different requirements from water based CEST imaging, and as a result has spurred new imaging methods to allow faster acquisition (107,108).

7. Outlook for the future of CEST imaging

One of the major criticisms pointed at CEST MRI is its low sensitivity. Indeed, CEST MRI would be more appealing for the broad imaging community if the sensitivity could be improved. Improving the robustness of the technology could be achieved through three independent levels: (1) better probe design, (2) better MRI imaging sequences and (3) increased reproducibility (Fig. 7). For example, CEST data are often contaminated by multiple components that interfere with detecting the probe of interest. We have developed an approach, termed Length and Offset VARied Saturation (LOVARS) (109), in which the length (t_{sat}) and $\Delta\omega$ of the saturation pulse is varied to modulate the water signal loss and impart differential phases on the interfering components. This allows their separation from the desired probe signal using post-processing techniques similar to those used to analyze

time-varying signal changes in event-related fMRI (110-116), such as Fast Fourier Transform (FFT) to separate different frequency components(109). Finally, it is key to repeatedly use the against with the highest standard of rigorous and reproducibility(117), in order to achieve highly sensitive, user-friendly imaging probe. Other approaches including systematic variation of saturation pulse flip angle, of multiple frequency pulses or variable delay elements and use of frequency labeling pulses instead of saturation or improvements in modeling the Z-spectra (118-123). CEST imaging sequence design is still relatively immature as a field, and the expectation is that many improvements in probe, sequence and post-processing will be forthcoming. As a result, molecular imaging using CEST should have a bright future.

References

1. Hancu I, Dixon WT, Woods M, Vinogradov E, Sherry AD, Lenkinski RE. CEST and PARACEST MR contrast agents. Acta Radiol. 2010; 51(8):910–923. [PubMed: 20828299]
2. Terreno E, Castelli DD, Aime S. Encoding the frequency dependence in MRI contrast media: the emerging class of CEST agents. Contrast Media and Molecular Imaging. 2010; 5(2):78–98. [PubMed: 20419761]
3. Wu YJL, Ye Q, Eytan DF, Liu L, Rosario BL, Hitchens TK, Yeh FC, van Rooijen N, Ho C. Magnetic Resonance Imaging Investigation of Macrophages in Acute Cardiac Allograft Rejection After Heart Transplantation. Circ-Cardiovasc Imaging. 2013; 6(6):965–973. [PubMed: 24097421]
4. van Zijl PC, Yadav NN. Chemical exchange saturation transfer (CEST): what is in a name and what isn't? Magn Reson Med. 2011; 65(4):927–948. [PubMed: 21337419]
5. Forsen S, Hoffman RA. STUDY OF MODERATELY RAPID CHEMICAL EXCHANGE REACTIONS BY MEANS OF NUCLEAR MAGNETIC DOUBLE RESONANCE. J Chem Phys. 1963; 39(11):2892–&.
6. Forsen S, Hoffman RA. A NEW METHOD FOR STUDY OF MODERATELY RAPID CHEMICAL EXCHANGE RATES EMPLOYING NUCLEAR MAGNETIC DOUBLE RESONANCE. Acta Chem Scand. 1963; 17(6):1787–&.
7. Wolff SD, Balaban RS. Nmr Imaging of Labile Proton-Exchange. J Magn Reson. 1990; 86(1):164–169.
8. Dagher AP, Aletras A, Choyke P, Balaban RS. Imaging of urea using chemical exchange-dependent saturation transfer at 1.5 T. J Magn Reson Imaging. 2000; 12(5):745–748. [PubMed: 11050645]
9. Chan KW, Liu G, Song X, Kim H, Yu T, Arifin DR, Gilad AA, Hanes J, Walczak P, van Zijl PC, Bulte JW, McMahon MT. MRI-detectable pH nanosensors incorporated into hydrogels for in vivo sensing of transplanted-cell viability. Nat Mater. 2013; 12(3):268–275. [PubMed: 23353626]
10. Dagher AP, Aletras A, Choyke P, Balaban RS. Imaging of urea using chemical exchange-dependent saturation transfer at 1.5T. Journal of magnetic resonance imaging : JMRI. 2000; 12(5): 745–748. [PubMed: 11050645]
11. Zhou J, Payen JF, Wilson DA, Traystman RJ, van Zijl PC. Using the amide proton signals of intracellular proteins and peptides to detect pH effects in MRI. Nat Med. 2003; 9(8):1085–1090. [PubMed: 12872167]
12. Zhou J, Lal B, Wilson DA, Laterra J, van Zijl PC. Amide proton transfer (APT) contrast for imaging of brain tumors. Magnetic resonance in medicine : official journal of the Society of Magnetic Resonance in Medicine / Society of Magnetic Resonance in Medicine. 2003; 50(6): 1120–1126.
13. Sun PZ, Zhou J, Sun W, Huang J, van Zijl PC. Suppression of lipid artifacts in amide proton transfer imaging. Magnetic resonance in medicine : official journal of the Society of Magnetic Resonance in Medicine / Society of Magnetic Resonance in Medicine. 2005; 54(1):222–225.
14. Gilad, AA.; McMahon, MT.; Winnard, PTJ.; Raman, V.; Bulte, JWM.; van Zijl, PCM. Developing a new class of CEST reporter genes.. The Fourth Annual Meeting of the Society for Molecular Imaging Conference; Cologne, Germany. Sept. 7-10, 2005;

15. Liu G, Moake M, Har-el Y-e, Long CM, Chan KWY, Cardona A, Jamil M, Walczak P, Gilad AA, Sgouros G, van Zijl PCM, Bulte JWM, McMahon MT. In vivo multicolor molecular MR imaging using diamagnetic chemical exchange saturation transfer liposomes. Magnetic Resonance in Medicine. 2012; 67(4):1106–1113. [PubMed: 22392814]
16. Liu G, Gilad AA, Bulte JWM, Van Zijl PCM, Mcmahon MT. High-throughput screening of chemical exchange saturation transfer MR contrast agents. Contrast Media and Molecular Imaging. 2010; 5(3):162–170. [PubMed: 20586030]
17. McMahon MT, Gilad AA, DeLiso MA, Cromer Berman SM, Bulte JWM, van Zijl PCM. New “multicolor” polypeptide diamagnetic chemical exchange saturation transfer (DIACEST) contrast agents for MRI. Magnetic Resonance in Medicine. 2008; 60(4):803–812. [PubMed: 18816830]
18. Viswanathan S, Ratnakar SJ, Green KN, Kovacs Z, De Leon-Rodriguez LM, Sherry AD. Multi-frequency PARACEST agents based on europium(III)-DOTA-tetraamide ligands. Angew Chem Int Ed Engl. 2009; 48(49):9330–9333. [PubMed: 19894248]
19. Norris DG. High field human imaging. J Magn Reson Imaging. 2003; 18(5):519–529. [PubMed: 14579394]
20. van Zijl PC, Jones CK, Ren J, Malloy CR, Sherry AD. MRI detection of glycogen in vivo by using chemical exchange saturation transfer imaging (glycoCEST). Proc Natl Acad Sci U S A. 2007; 104(11):4359–4364. [PubMed: 17360529]
21. Chan KW, McMahon MT, Kato Y, Liu G, Bulte JW, Bhujwalla ZM, Artemov D, van Zijl PC. Natural D-glucose as a biodegradable MRI contrast agent for detecting cancer. Magnetic resonance in medicine : official journal of the Society of Magnetic Resonance in Medicine / Society of Magnetic Resonance in Medicine. 2012; 68(6):1764–1773.
22. Nasrallah FA, Pages G, Kuchel PW, Golay X, Chuang KH. Imaging brain deoxyglucose uptake and metabolism by glucoCEST MRI. Journal of cerebral blood flow and metabolism : official journal of the International Society of Cerebral Blood Flow and Metabolism. 2013; 33(8):1270–1278.
23. Singh A, Cai K, Haris M, Hariharan H, Reddy R. On B1 inhomogeneity correction of in vivo human brain glutamate chemical exchange saturation transfer contrast at 7T. Magnetic resonance in medicine : official journal of the Society of Magnetic Resonance in Medicine / Society of Magnetic Resonance in Medicine. 2013; 69(3):818–824.
24. Cai K, Haris M, Singh A, Kogan F, Greenberg JH, Hariharan H, Detre JA, Reddy R. Magnetic resonance imaging of glutamate. Nat Med. 2012; 18(2):302–306. [PubMed: 22270722]
25. Kogan F, Haris M, Singh A, Cai K, Debrosse C, Nanga RPR, Hariharan H, Reddy R. Method for high-resolution imaging of creatine in vivo using chemical exchange saturation transfer. Magnetic Resonance in Medicine. 2013:n/a–n/a.
26. Liu G, Moake M, Har-el YE, Long CM, Chan KW, Cardona A, Jamil M, Walczak P, Gilad AA, Sgouros G, van Zijl PC, Bulte JW, McMahon MT. In vivo multicolor molecular MR imaging using diamagnetic chemical exchange saturation transfer liposomes. Magnetic resonance in medicine : official journal of the Society of Magnetic Resonance in Medicine / Society of Magnetic Resonance in Medicine. 2012; 67(4):1106–1113.
27. Yang X, Yadav NN, Song X, Ray Banerjee S, Edelman H, Minn I, van Zijl PC, Pomper MG, McMahon MT. Tuning phenols with Intra-Molecular bond Shifted HYdrogens (IM-SHY) as diaCEST MRI contrast agents. Chemistry. 2014; 20(48):15824–15832. [PubMed: 25302635]
28. Yu T, Chan KW, Anonuevo A, Song X, Schuster BS, Chattopadhyay S, Xu Q, Oskolkov N, Patel H, Ensign LM, van Zjil PC, McMahon MT, Hanes J. Liposome-based mucus-penetrating particles (MPP) for mucosal theranostics: demonstration of diamagnetic chemical exchange saturation transfer (diaCEST) magnetic resonance imaging (MRI). Nanomedicine. 2015; 11(2):401–405. [PubMed: 25461289]
29. Lee, JS.; Xia, D.; Parasoglou, P.; Chang, G.; Jerschow, A.; Regatte, RR. Chemical exchange saturation transfer contrast by glycosaminoglycans and its application for monitoring knee joint repair. Regatte, RR., editor. World Scientific Publ Co Pte Ltd; Singapore: 2014. p. 249-271.
30. Bar-Shir A, Liu GS, Liang YJ, Yadav NN, McMahon MT, Walczak P, Nimmagadda S, Pomper MG, Tallman KA, Greenberg MM, van Zijl PCM, Bulte JWM, Gilad AA. Transforming Thymidine into a Magnetic Resonance Imaging Probe for Monitoring Gene Expression. J Am Chem Soc. 2013; 135(4):1617–1624. [PubMed: 23289583]

31. Wu RH, Longo DL, Aime S, Sun PZ. Quantitative description of radiofrequency (RF) power-based ratiometric chemical exchange saturation transfer (CEST) pH imaging. NMR Biomed. 2015; 28(5):555–565. [PubMed: 25807919]
32. Longo DL, Dastru W, Digilio G, Keupp J, Langereis S, Lanzardo S, Prestigio S, Steinbach O, Terreno E, Uggeri F, Aime S. Iopamidol as a Responsive MRI-Chemical Exchange Saturation Transfer Contrast Agent for pH Mapping of Kidneys: In Vivo Studies in Mice at 7 T. Magnetic Resonance in Medicine. 2011; 65(1):202–211. [PubMed: 20949634]
33. Chen LQ, Howison CM, Jeffery JJ, Robey IF, Kuo PH, Pagel MD. Evaluations of extracellular pH within in vivo tumors using acidoCEST MRI. Magnetic Resonance in Medicine. 2013:n/a–n/a.
34. Yang X, Song X, Ray Banerjee S, Li Y, Byun Y, Liu G, Bhujwalla ZM, Pomper MG, McMahon MT. Developing imidazoles as CEST MRI pH sensors. Contrast Media Mol Imaging. 2016
35. Mock WL, Morsch LA. Low barrier hydrogen bonds within salicylate mono-anions. Tetrahedron. 2001; 57(15):2957–2964.
36. Maciel GE, Savitsky GB. CARBON - 13 CHEMICAL SHIFTS + INTRAMOLECULAR HYDROGEN BONDING. Journal of Physical Chemistry. 1964; 68(2):437–&.
37. Li J, Feng X, Zhu W, Oskolkov N, Zhou T, Kim BK, Baig N, McMahon MT, Oldfield E. Chemical Exchange Saturation Transfer (CEST) Agents: Quantum Chemistry and MRI. Chemistry. 2016; 22(1):264–271. [PubMed: 26616530]
38. Song X, Walczak P, He X, Yang X, Pearl M, Bulte JW, Pomper MG, McMahon MT, Janowski M. Salicylic acid analogues as chemical exchange saturation transfer MRI contrast agents for the assessment of brain perfusion territory and blood-brain barrier opening after intra-arterial infusion. J Cereb Blood Flow Metab. 2016; 36(7):1186–1194. [PubMed: 26980755]
39. Xu X, Yadav NN, Knutsson L, Hua J, Kalyani R, Hall E, Laterra J, Blakeley J, Strowd R, Pomper M, Barker P, Chan K, Liu G, McMahon MT, Stevens RD, van Zijl PCM. Dynamic Glucose-Enhanced (DGE) MRI: Translation to Human Scanning and First Results in Glioma Patients. Tomography : a journal for imaging research. 2015; 1(2):105–114. [PubMed: 26779568]
40. Muller-Lutz A, Khalil N, Schmitt B, Jellus V, Pentang G, Oeltzschner G, Antoch G, Lanzman RS, Wittsack HJ. Pilot study of Iopamidol-based quantitative pH imaging on a clinical 3T MR scanner. MAGMA. 2014; 27(6):477–485. [PubMed: 24570337]
41. Zhang S, Merritt M, Woessner DE, Lenkinski RE, Sherry AD. PARACEST Agents: Modulating MRI Contrast via Water Proton Exchange. Acc Chem Res. 2003; 36:783–790. [PubMed: 14567712]
42. Zhang S, Winter P, Wu K, Sherry AD. A novel europium(III)-based MRI contrast agent. J Am Chem Soc. 2001; 123(7):1517–1518. [PubMed: 11456734]
43. Aime S, Barge A, Delli Castelli D, Fedeli F, Mortillaro A, Nielsen FU, Terreno E. Paramagnetic lanthanide(III) complexes as pH-sensitive chemical exchange saturation transfer (CEST) contrast agents for MRI applications. Magn Reson Med. 2002; 47(4):639–648. [PubMed: 11948724]
44. Aime S, Delli Castelli D, Fedeli F, Terreno E. A paramagnetic MRI-CEST agent responsive to lactate concentration. J Am Chem Soc. 2002; 124(32):9364–9365. [PubMed: 12167018]
45. Yoo B, Pagel MD. A PARACEST MRI contrast agent to detect enzyme activity. J Am Chem Soc. 2006; 128(43):14032–14033. [PubMed: 17061878]
46. Yoo B, Pagel MD. An overview of responsive MRI contrast agents for molecular imaging. Front Biosci. 2008; 13:1733–1752. [PubMed: 17981664]
47. Li AX, Wojciechowski F, Suchy M, Jones CK, Hudson RHE, Merton RS, Bartha R. A sensitive PARACEST contrast agent for temperature MRI: EU3+-DOTAM-Glycine (Gly)-Phenylalanine (Phe). Magn Reson Med. 2008; 59(2):374–381. [PubMed: 18228602]
48. Dorazio SJ, Tsitovich PB, Siters KE, Spernyak JA, Morrow JR. Iron(II) PARACEST MRI Contrast Agents. J Am Chem Soc. 2011; 133(36):14154–14156. [PubMed: 21838276]
49. Tsitovich PB, Spernyak JA, Morrow JR. A Redox-Activated MRI Contrast Agent that Switches Between Paramagnetic and Diamagnetic States. Angew Chem-Int Edit. 2013; 52(52):13997–14000.
50. Angelovski G, Chauvin T, Pohmann R, Logothetis NK, Toth E. Calcium-responsive paramagnetic CEST agents. Bioorg Med Chem. 2011; 19(3):1097–1105. [PubMed: 20691598]

51. Cakic N, Savic T, Stricker-Shaver J, Truffault V, Platas-Iglesias C, Mirkes C, Pohmann R, Scheffler K, Angelovski G. Paramagnetic lanthanide chelates for multicontrast MRI. Chem Commun (Camb). 2016; 52(59):9224–9227. [PubMed: 27291157]
52. Cakic N, Verbic TZ, Jelic RM, Platas-Iglesias C, Angelovski G. Synthesis and characterisation of bismacrocyclic DO3A-amide derivatives - an approach towards metal-responsive PARACEST agents. Dalton Trans. 2016; 45(15):6555–6565. [PubMed: 26956151]
53. Terreno E, Castelli DD, Aime S. Encoding the frequency dependence in MRI contrast media: the emerging class of CEST agents. Contrast Media Mol Imaging. 2010; 5(2):78–98. [PubMed: 20419761]
54. Yoo B, Pagel MD. A PARACEST MRI contrast agent to detect enzyme activity. J Am Chem Soc. 2006; 128(43):14032–14033. [PubMed: 17061878]
55. Dorazio SJ, Tsitovich PB, Siters KE, Spernyak JA, Morrow JR. Iron(II) PARACEST MRI Contrast Agents. J Am Chem Soc. 2011; 133(36):14154–14156. [PubMed: 21838276]
56. Olatunde AO, Dorazio SJ, Spernyak JA, Morrow JR. The NiCEST Approach: Nickel(II) ParaCEST MRI Contrast Agents. J Am Chem Soc. 2012; 134(45):18503–18505. [PubMed: 23102112]
57. Dorazio SJ, Olatunde AO, Spernyak JA, Morrow JR. CoCEST: cobalt(II) amide-appended paraCEST MRI contrast agents. Chem Commun. 2013; 49(85):10025–10027.
58. Rancan G, Delli Castelli D, Aime S. MRI CEST at 1T with large microeff Ln(3+) complexes T m(3+)-HPDO3A: An efficient MRI pH reporter. Magn Reson Med. 2016; 75(1):329–336. [PubMed: 25651986]
59. Penet M-F, Artemov D, Farahani K, Bhujwalla ZM. MR – eyes for cancer: looking within an impenetrable disease. NMR in Biomedicine. 2013; 26(7):745–755. [PubMed: 23784955]
60. Lesniak WG, Oskolkov N, Song X, Lal B, Yang X, Pomper M, Laterra J, Nimmagadda S, McMahon MT. Salicylic Acid Conjugated Dendrimers Are a Tunable, High Performance CEST MRI NanoPlatform. Nano Lett. 2016; 16(4):2248–2253. [PubMed: 26910126]
61. Winter PM, Cai K, Chen J, Adair CR, Kiefer GE, Athey PS, Gaffney PJ, Buff CE, Robertson JD, Caruthers SD, Wickline SA, Lanza GM. Targeted PARACEST nanoparticle contrast agent for the detection of fibrin. Magn Reson Med. 2006; 56(6):1384–1388. [PubMed: 17089356]
62. Pikkemaat JA, Wegh RT, Lamerichs R, van de Molengraaf RA, Langereis S, Burdinski D, Raymond AYF, Janssen HM, de Waal BFM, Willard NP, Meijer EW, Grull H. Dendritic PARACEST contrast agents for magnetic resonance imaging. Contrast Media Mol Imaging. 2007; 2(5):229–239. [PubMed: 17937448]
63. Ali MM, Liu GS, Shah T, Flask CA, Pagel MD. Using Two Chemical Exchange Saturation Transfer Magnetic Resonance Imaging Contrast Agents for Molecular Imaging Studies. Accounts Chem Res. 2009; 42(7):915–924.
64. Aime S, Delli Castelli D, Terreno E. Highly Sensitive MRI Chemical Exchange Saturation Transfer Agents Using Liposomes. Angewandte Chemie International Edition. 2005; 44(34):5513–5515.
65. Flament J, Geffroy F, Medina C, Robic C, Mayer JF, Meriaux S, Valette J, Robert P, Port M, Le Bihan D, Lethimonnier F, Boumezbeur F. In vivo CEST MR imaging of U87 mice brain tumor angiogenesis using targeted LipoCEST contrast agent at 7 T. Magn Reson Med. 2013; 69(1):179–187. [PubMed: 22378016]
66. Ngen EJ, Bar-Shir A, Jablonska A, Liu G, Song X, Ansari R, Bulte JW, Janowski M, Pearl M, Walczak P, Gilad AA. Imaging the DNA Alkylator Melphalan by CEST MRI: An Advanced Approach to Theranostics. Mol Pharm. 2016
67. Goffeney N, Bulte JW, Duyn J, Bryant LH Jr. van Zijl PC. Sensitive NMR detection of cationic-polymer-based gene delivery systems using saturation transfer via proton exchange. J Am Chem Soc. 2001; 123(35):8628–8629. [PubMed: 11525684]
68. Liu G, Gilad AA, Bulte JW, van Zijl PC, McMahon MT. High-throughput screening of chemical exchange saturation transfer MR contrast agents. Contrast Media Mol Imaging. 2010; 5(3):162–170. [PubMed: 20586030]
69. McMahon MT, Gilad AA, Zhou J, Sun PZ, Bulte JW, van Zijl PC. Quantifying exchange rates in chemical exchange saturation transfer agents using the saturation time and saturation power dependencies of the magnetization transfer effect on the magnetic resonance imaging signal

(QUEST and QUESP): Ph calibration for poly-L-lysine and a starburst dendrimer. Magn Reson Med. 2006; 55(4):836–847. [PubMed: 16506187]

70. Petrone J. DNA writers attract investors. Nat Biotech. 2016; 34(4):363–364.
71. Airan RD, Bar-Shir A, Liu G, Pelled G, McMahon MT, van Zijl PC, Bulte JW, Gilad AA. MRI biosensor for protein kinase A encoded by a single synthetic gene. Magn Reson Med. 2012; 68(6): 1919–1923. [PubMed: 23023588]
72. Bar-Shir A, Bulte JW, Gilad AA. Molecular Engineering of Nonmetallic Biosensors for CEST MRI. ACS Chem Biol. 2015
73. Bar-Shir A, Liang Y, Chan KW, Gilad AA, Bulte JW. Supercharged green fluorescent proteins as bimodal reporter genes for CEST MRI and optical imaging. Chem Commun (Camb). 2015; 51(23):4869–4871. [PubMed: 25697683]
74. Bar-Shir A, Liu G, Chan KW, Oskolkov N, Song X, Yadav NN, Walczak P, McMahon MT, van Zijl PC, Bulte JW, Gilad AA. Human protamine-1 as an MRI reporter gene based on chemical exchange. ACS Chem Biol. 2014; 9(1):134–138. [PubMed: 24138139]
75. Oskolkov N, Bar-Shir A, Chan KWY, Song X, van Zijl PCM, Bulte JWM, Gilad AA, McMahon MT. Biophysical Characterization of Human Protamine-1 as a Responsive CEST MR Contrast Agent. ACS Macro Letters. 2014:34–38. [PubMed: 25642384]
76. Gilad AA, McMahon MT, Walczak P, Winnard PT Jr. Raman V, van Laarhoven HW, Skoglund CM, Bulte JW, van Zijl PC. Artificial reporter gene providing MRI contrast based on proton exchange. Nat Biotechnol. 2007; 25(2):217–219. [PubMed: 17259977]
77. Bar-Shir A, Liu G, Liang Y, Yadav NN, McMahon MT, Walczak P, Nimmagadda SR, Pomper MG, Tallman KA, Greenberg MM, van Zijl PC, Bulte JW, Gilad AA. Transforming thymidine into a magnetic resonance imaging probe for monitoring gene expression. J Am Chem Soc. 2013; 135(4):1617–1624. [PubMed: 23289583]
78. Farrar CT, Buhrman JS, Liu G, Kleijn A, Lamfers ML, McMahon MT, Gilad AA, Fulci G. Establishing the lysine-rich protein CEST reporter gene as a CEST-MRI detector for oncolytic virotherapy. Radiology. 2015 In press.
79. Minn I, Bar-Shir A, Yarlagadda K, Bulte JWM, Fisher PB, Wang H, Gilad AA, Pomper MG. Tumor-specific expression and detection of a CEST reporter gene. Magnetic Resonance in Medicine. 2015; 74(2):544–549. [PubMed: 25919119]
80. Aime S, Calabi L, Biondi L, De Miranda M, Ghelli S, Paleari L, Rebaudengo C, Terreno E. Iopamidol: Exploring the potential use of a well-established X-ray contrast agent for MRI. Magnetic Resonance in Medicine. 2005; 53(4):830–834. [PubMed: 15799043]
81. McMahon MT, Gilad AA, DeLiso MA, Berman SM, Bulte JW, van Zijl PC. New “multicolor” polypeptide diamagnetic chemical exchange saturation transfer (DIACEST) contrast agents for MRI. Magn Reson Med. 2008; 60(4):803–812. [PubMed: 18816830]
82. Esqueda AC, Lopez JA, Andreu-de-Riquer G, Alvarado-Monzon JC, Ratnakar J, Lubag AJ, Sherry AD, De Leon-Rodriguez LM. A new gadolinium-based MRI zinc sensor. J Am Chem Soc. 2009; 131(32):11387–11391. [PubMed: 19630391]
83. Lubag AJ, De Leon-Rodriguez LM, Burgess SC, Sherry AD. Noninvasive MRI of beta-cell function using a Zn2+-responsive contrast agent. Proc Natl Acad Sci U S A. 2011; 108(45): 18400–18405. [PubMed: 22025712]
84. Bar-Shir A, Yadav NN, Gilad AA, van Zijl PC, McMahon MT, Bulte JW. Single (19)F probe for simultaneous detection of multiple metal ions using miCEST MRI. J Am Chem Soc. 2015; 137(1): 78–81. [PubMed: 25523816]
85. Bar-Shir A, Gilad AA, Chan KW, Liu G, van Zijl PC, Bulte JW, McMahon MT. Metal ion sensing using ion chemical exchange saturation transfer 19F magnetic resonance imaging. J Am Chem Soc. 2013; 135(33):12164–12167. [PubMed: 23905693]
86. Chan KWY, Liu G, Song X, Kim H, Yu T, Arifin DR, Gilad AA, Hanes J, Walczak P, van Zijl PCM, Bulte JWM, McMahon MT. MRI-detectable pH nanosensors incorporated into hydrogels for in vivo sensing of transplanted-cell viability. Nature materials. 2013; 12(3):268–275. [PubMed: 23353626]
87. Shrode LD, Tapper H, Grinstein S. Role of intracellular pH in proliferation, transformation, and apoptosis. J Bioenerg Biomembr. 1997; 29(4):393–399. [PubMed: 9387100]

88. Barnett BP, Arepally A, Karmarkar PV, Qian D, Gilson WD, Walczak P, Howland V, Lawler L, Lauzon C, Stuber M, Kraitchman DL, Bulte JW. Magnetic resonance-guided, real-time targeted delivery and imaging of magnetocapsules immunoprotecting pancreatic islet cells. Nat Med. 2007; 13(8):986–991. [PubMed: 17660829]

89. Barnett BP, Ruiz-Cabello J, Hota P, Liddell R, Walczak P, Howland V, Chacko VP, Kraitchman DL, Arepally A, Bulte JW. Fluorocapsules for improved function, immunoprotection, and visualization of cellular therapeutics with MR, US, and CT imaging. Radiology. 2011; 258(1): 182–191. [PubMed: 20971778]

90. Chan KW, Liu G, Song X, Kim H, Yu T, Arifin DR, Gilad AA, Hanes J, Walczak P, van Zijl PC, Bulte JW, McMahon MT. MRI-detectable pH nanosensors incorporated into hydrogels for in vivo sensing of transplanted-cell viability. Nature materials. 2013; 12(3):268–275. [PubMed: 23353626]

91. Chan KWY, Liu GS, van Zijl PCM, Bulte JWM, McMahon MT. Magnetization transfer contrast MRI for non-invasive assessment of innate and adaptive immune responses against alginate-encapsulated cells. Biomaterials. 2014; 35(27):7811–7818. [PubMed: 24930848]

92. Schroder L, Lowery TJ, Hilty C, Wemmer DE, Pines A. Molecular imaging using a targeted magnetic resonance hyperpolarized biosensor. Science. 2006; 314(5798):446–449. [PubMed: 17053143]

93. Amor N, Zanker PP, Blumler P, Meise FM, Schreiber LM, Scholz A, Schmiedeskamp J, Spiess HW, Munnemann K. Magnetic resonance imaging of dissolved hyperpolarized Xe-129 using a membrane-based continuous flow system. J Magn Reson. 2009; 201(1):93–99. [PubMed: 19729327]

94. Chen RYZ, Fan FC, Kim S, Jan KM, Usami S, Chien S. TISSUE-BLOOD PARTITION-COEFFICIENT FOR XENON - TEMPERATURE AND HEMATOCRIT DEPENDENCE. J Appl Physiol. 1980; 49(2):178–183. [PubMed: 7400000]

95. Swanson SD, Rosen MS, Coulter KP, Welsh RC, Chupp TE. Distribution and dynamics of laser-polarized (129)Xe magnetization in vivo. Magnetic resonance in medicine : official journal of the Society of Magnetic Resonance in Medicine / Society of Magnetic Resonance in Medicine. 1999; 42(6):1137–1145.

96. Nikolaou P, Coffey AM, Walkup LL, Gust BM, Whiting N, Newton H, Muradyan I, Dabaghyan M, Ranta K, Moroz GD, Rosen MS, Patz S, Barlow MJ, Chekmenev EY, Goodson BM. XeNA: An automated 'open-source' Xe-129 hyperpolarizer for clinical use. Magn Reson Imaging. 2014; 32(5):541–550. [PubMed: 24631715]

97. Goodson BM. Nuclear magnetic resonance of laser-polarized noble gases in molecules, materials, and organisms. J Magn Reson. 2002; 155(2):157–216. [PubMed: 12036331]

98. Nikolaou P, Coffey AM, Walkup LL, Gust BM, Whiting N, Newton H, Barcus S, Muradyan I, Dabaghyan M, Moroz GD, Rosen MS, Patz S, Barlow MJ, Chekmenev EY, Goodson BM. Near-unity nuclear polarization with an open-source Xe-129 hyperpolarizer for NMR and MRI. Proc Natl Acad Sci U S A. 2013; 110(35):14150–14155. [PubMed: 23946420]

99. Rosen MS, Chupp TE, Coulter KP, Welsh RC, Swanson SD. Polarized Xe-129 optical pumping/spin exchange and delivery system for magnetic resonance spectroscopy and imaging studies. Rev Sci Instrum. 1999; 70(2):1546–1552.

100. Tassali N, Kotera N, Boutin C, Leonce E, Boulard Y, Rousseau B, Dubost E, Taran F, Brotin T, Dutasta JP, Berthauet P. Smart Detection of Toxic Metal Ions, Pb2+ and Cd2+, Using a Xe-129 NMR-Based Sensor. Anal Chem. 2014; 86(3):1783–1788. [PubMed: 24432871]

101. Zhang J, Jiang WP, Luo Q Zhang XX, Guo QN, Liu ML, Zhou X. Rational design of hyperpolarized xenon NMR molecular sensor for the selective and sensitive determination of zinc ions. Talanta. 2014; 122:101–105. [PubMed: 24720969]

102. Guo QN, Zeng QB, Jiang WP, Zhang XX, Luo Q, Zhang X, Bouchard LS, Liu ML, Zhou X. A Molecular Imaging Approach to Mercury Sensing Based on Hyperpolarized Xe-129 Molecular Clamp Probe. Chem-Eur J. 2016; 22(12):3967–3970. [PubMed: 26792102]

103. Stevens TK, Palaniappan KK, Ramirez RM, Francis MB, Wemmer DE, Pines A. HyperCEST detection of a 129Xe-based contrast agent composed of cryptophane-A molecular cages on a bacteriophage scaffold. Magnetic Resonance in Medicine. 2013; 69(5):1245–1252. [PubMed: 22791581]

104. Klippel S, Dopfert J, Jayapaul J, Kunth M, Rossella F, Schnurr M, Witte C, Freund C, Schroder L. Cell Tracking with Caged Xenon: Using Cryptophanes as MRI Reporters upon Cellular Internalization. Angewandte Chemie-International Edition. 2014; 53(2):493–496.
105. Shapiro MG, Ramirez RM, Sperling LJ, Sun G, Sun J, Pines A, Schaffer DV, Bajaj VS. Genetically encoded reporters for hyperpolarized xenon magnetic resonance imaging. Nat Chem. 2014; 6(7):630–635.
106. Bai YB, Wang YF, Goulian M, Driks A, Dmochowski IJ. Bacterial spore detection and analysis using hyperpolarized Xe-129 chemical exchange saturation transfer (Hyper-CEST) NMR. Chem Sci. 2014; 5(8):3197–3203. [PubMed: 25089181]
107. Dopfert J, Witte C, Schroder L. Fast Gradient-Encoded CEST Spectroscopy of Hyperpolarized Xenon. Chemphyschem. 2014; 15(2):261–264. [PubMed: 24408772]
108. Dopfert J, Witte C, Kunth M, Schroder L. Sensitivity enhancement of (Hyper-)CEST image series by exploiting redundancies in the spectral domain. Contrast Media Mol Imaging. 2014; 9(1):100–107. [PubMed: 24470299]
109. Song X, Gilad AA, Joel S, Liu G, Bar-Shir A, Liang Y, Gorelik M, Pekar JJ, van Zijl PC, Bulte JW, McMahon MT. CEST phase mapping using a length and offset varied saturation (LOVARS) scheme. Magn Reson Med. 2012; 68(4):1074–1086. [PubMed: 22246684]
110. Bandettini PA, Jesmanowicz A, Wong EC, Hyde JS. Processing Strategies for Time-Course Data Sets in Functional Mri of the Human Brain. Magnetic Resonance in Medicine. 1993; 30(2):161–173. [PubMed: 8366797]
111. Cox RW. AFNI: software for analysis and visualization of functional magnetic resonance neuroimages. Comput Biomed Res. 1996; 29(3):162–173. [PubMed: 8812068]
112. McKeown MJ, Makeig S, Brown GG, Jung TP, Kindermann SS, Bell AJ, Sejnowski TJ. Analysis of fMRI data by blind separation into independent spatial components. Human Brain Mapping. 1998; 6(3):160–188. [PubMed: 9673671]
113. Cohen MS. Parametric analysis of fMRI data using linear systems methods. Neuroimage. 1997; 6(2):93–103. [PubMed: 9299383]
114. Friston KJ, Holmes AP, Worsley KJ, Poline JP, Frith CD, Frackowiak RSJ. Statistical parametric maps in functional imaging: A general linear approach. Human Brain Mapping. 1994; 2(4):189–210.
115. Calhoun VD, Adali T, Pearlson GD, Pekar JJ. Spatial and temporal independent component analysis of functional MRI data containing a pair of task-related waveforms. Human Brain Mapping. 2001; 13(1):43–53. [PubMed: 11284046]
116. Smith SM, Jenkinson M, Woolrich MW, Beckmann CF, Behrens TEJ, Johansen-Berg H, Bannister PR, De Luca M, Drobnjak I, Flitney DE, Niazy RK, Saunders J, Vickers J, Zhang YY, De Stefano N, Brady JM, Matthews PM. Advances in functional and structural MR image analysis and implementation as FSL. Neuroimage. 2004; 23:S208–S219. [PubMed: 15501092]
117. Landis SC, Amara SG, Asadullah K, Austin CP, Blumenstein R, Bradley EW, Crystal RG, Darnell RB, Ferrante RJ, Fillit H, Finkelstein R, Fisher M, Gendelman HE, Golub RM, Goudreau JL, Gross RA, Gubitz AK, Hesterlee SE, Howells DW, Huguenard J, Kelner K, Koroshetz W, Krainc D, Lazic SE, Levine MS, Macleod MR, McCall JM, Moxley RT 3rd, Narasimhan K, Noble LJ, Perrin S, Porter JD, Steward O, Unger E, Utz U, Silberberg SD. A call for transparent reporting to optimize the predictive value of preclinical research. Nature. 2012; 490(7419):187–191. [PubMed: 23060188]
118. Friedman JI, McMahon MT, Stivers JT, Van Zijl PC. Indirect detection of labile solute proton spectra via the water signal using frequency-labeled exchange (FLEX) transfer. J Am Chem Soc. 2010; 132(6):1813–1815. [PubMed: 20095603]
119. Xu J, Yadav NN, Bar-Shir A, Jones CK, Chan KWY, Zhang J, Walczak P, McMahon MT, van Zijl PCM. Variable delay multi-pulse train for fast chemical exchange saturation transfer and relayed-nuclear overhauser enhancement MRI. Magn Reson Med. 2014; 71(5):1798–1812. [PubMed: 23813483]
120. Yadav NN, Jones CK, Xu J, Bar-Shir A, Gilad AA, McMahon MT, van Zijl PC. Detection of rapidly exchanging compounds using on-resonance frequency-labeled exchange (FLEX) transfer. Magn Reson Med. 2012; 68(4):1048–1055. [PubMed: 22837066]

121. Lee JS, Regatte RR, Jerschow A. Isolating chemical exchange saturation transfer contrast from magnetization transfer asymmetry under two-frequency rf irradiation. J Magn Reson. 2012; 215:56–63. [PubMed: 22237631]

122. Zu ZL, Xu JZ, Li H, Chekmenev EY, Quarles CC, Does MD, Gore JC, Gochberg DF. Imaging Amide Proton Transfer and Nuclear Overhauser Enhancement Using Chemical Exchange Rotation Transfer (CERT). Magnetic Resonance in Medicine. 2014; 72(2):471–476. [PubMed: 24302497]

123. Zaiss M, Schmitt B, Bachert P. Quantitative separation of CEST effect from magnetization transfer and spillover effects by Lorentzian-line-fit analysis of z-spectra. J Magn Reson. 2011; 211(2):149–155. [PubMed: 21641247]

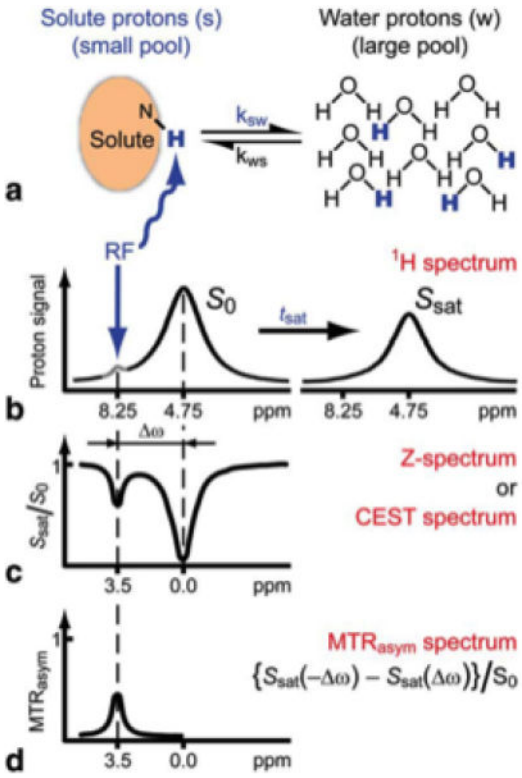

Figure 1.

Schematic of Chemical exchange saturation transfer (CEST): principles and measurement approach for pure exchange effects. **a, b)** Solute protons (blue) are saturated at their specific resonance frequency in the proton spectrum (here 8.25 ppm for amide protons). This saturation is transferred to water (4.75 ppm) at exchange rate k_{sw} and nonsaturated protons (black) return. After a period (t_{sat}), this effect becomes visible on the water signal (**b**, right). **c)** Measurement of normalized water saturation (S_{sat}/S_0) as a function of irradiation frequency, generating a so-called Z-spectrum (or CEST spectrum or MT spectrum). When irradiating the water protons at 4.75 ppm, the signal disappears due to direct (water) saturation (DS). This frequency is assigned to 0 ppm in Z-spectra. At short saturation times, only this direct saturation is apparent. At longer t_{sat} the CEST effect becomes visible at the frequency of the low- concentration exchangeable solute protons, now assigned to 8.25 - 4.75 = 3.5 ppm in the Z-spectrum. **d)** result of magnetization transfer ratio asymmetry analysis of the Z-spectrum with respect to the water frequency to remove the effect of direct saturation. Reproduced from (4) with permission.

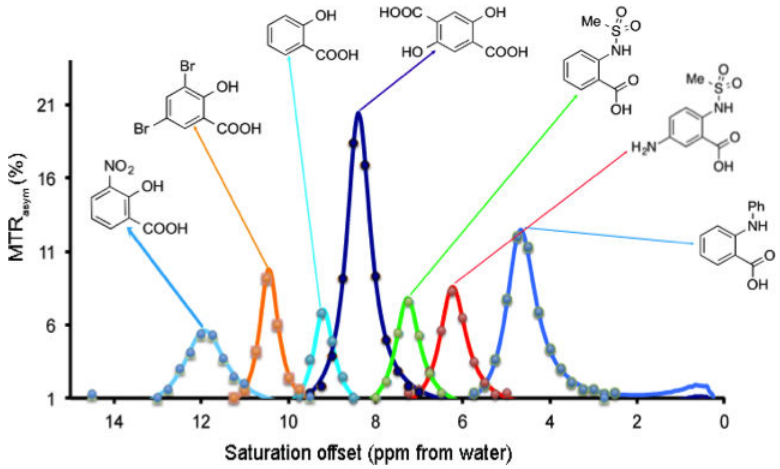

Figure 2.

Representative examples of IM-SHY CEST agents with tunable exchangeable protons. Conditions: CEST data were obtained at 17.6 T using 10 mM concentrations, pH 7.3 - 7.4, t_{sat} = 3 sec, ω_1 = 3.6 μT and T= 37 °C. Experimental data are shown as closed circles, while the lines represent Bloch simulations. Reproduced from (27) with permission.

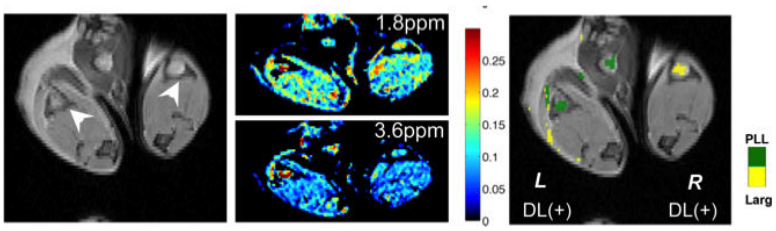

Figure 3.

Representative two-color CEST image demonstrating simultaneous detection and visualization after injection of L-arginine CEST liposomes and poly-l-ysine CEST liposomes into the footpads of a mouse. Left panel: T2-weighted anatomical image with arrows indicating the location of popliteal lymph nodes; Middle panel: MTR_{asym} images at the frequency of interest for L-arginine (1.8 ppm, upper) and poly-L-lysine (3.6 ppm lower); Right panel: MTR_{asym}/T2w image overlay with CEST contrast highlighted using a 64-bit scaled single color of PLL (green, left lymph node) and L-Arg (yellow, right lymph node). Reproduced from (26) with permission.

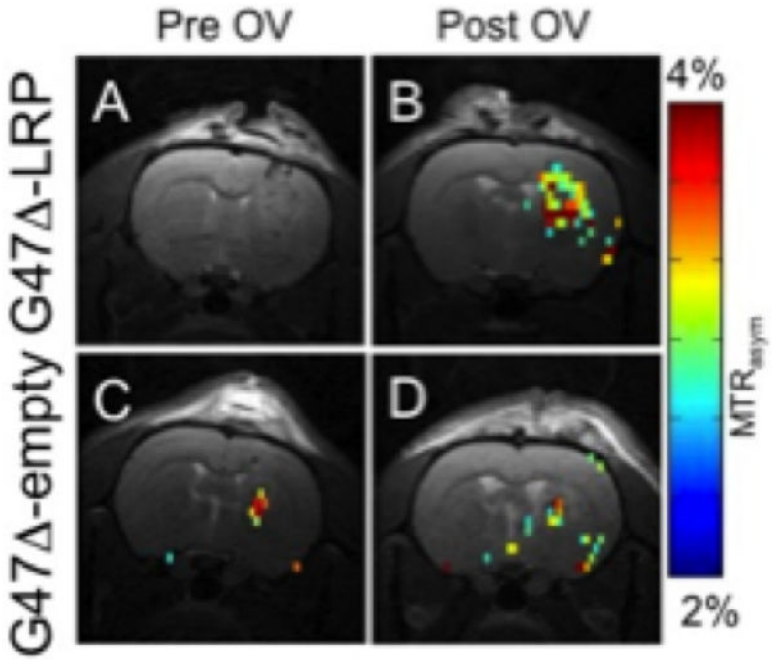

Figure 4. LRP In vivo

A & C) before and B & D) after injection of LRP-expressing oncolytic virus into a brain tumor in a live rat brain. There is a significant (p=0.05) increase in tumor CEST contrast for G47Δ-LRP (n=7) than for controls G47Δ-empty (n=6). Reproduced from (78) with permission.

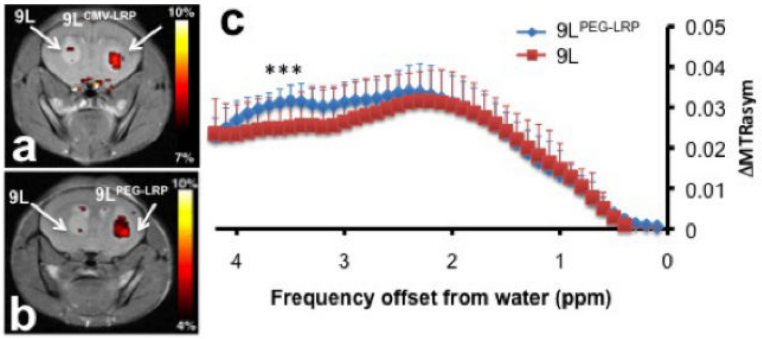

Figure 5.

a, b) Representative CEST maps superimposed on T2-weighted images:Left hemisphere has 9L tumors and right hemisphere has (a) $9L^{CMV\text{-}LRP}$ and (b) $9L^{PEG\text{-}LRP}$. c) Temporal changes in the ΔMTR_{asym} values (mean ± s.d.; 8 mice) of each tumor type. t-test showed statistical difference of CEST contrast at 3.4-3.6 ppm, (*$p<0.05$; n=8). Reproduced from (79) with permission.

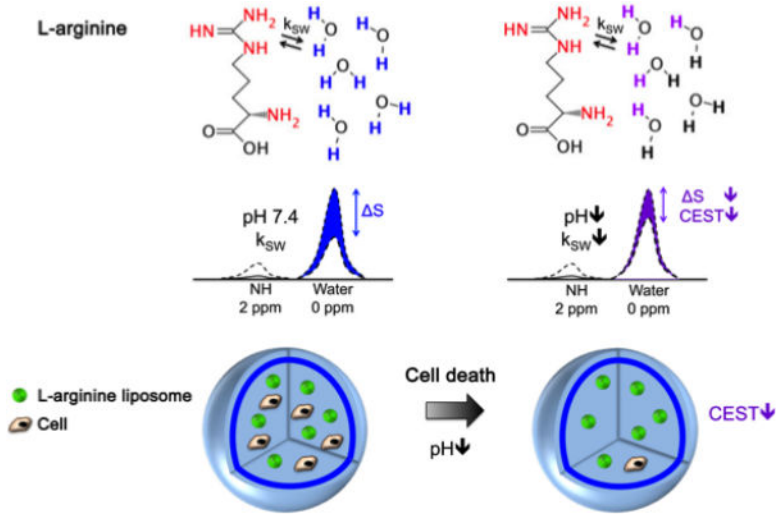

Figure 6. Schematic showing the principles of *in vivo* detection of cell viability using LipoCEST microcapsules as pH nanosensors

The CEST contrast is measured by the drop in the signal intensity (ΔS) of water after selective saturation (i.e. removal of capability to generate signal) of the NH protons in L-arginine at 2 ppm. The L-arginine protons (red) inside the LipoCEST capsules exchange (k_{SW}) with the surrounding water protons. The k_{SW} is reduced at lower pH causing a significant drop in CEST contrast. Reproduced from (9) with permission.

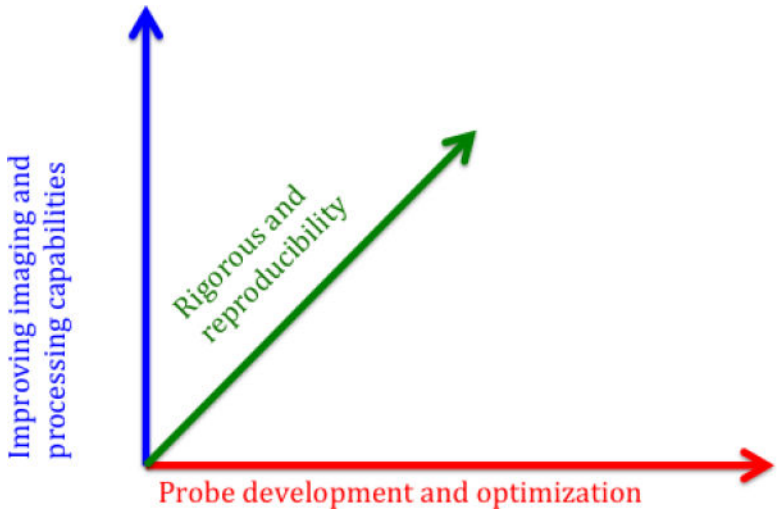

Figure 7.
Multi-dimensional development of molecular imaging using CEST.

Table 1

selected milestones in the developing of protein based CEST agents

	Authors	Year	Topic	Findings relevant to the next gen LRP	Ref.
1	McMahon et. al.	2008	Quantifying exchange rate	Determining the k_{ex} of exchangeable protons	(70)
2	Gilad et. al.	2007	LRP prototype	LRP can be expressed in the brain	(77)
3	McMahon et. al.	2008	Multicolor peptides	Changing the amino acid sequence affect the resonances frequency and the contrast intensity	(82)
4	Liu et. al.	2010	Peptide screening with MRI	Developing tools for high-throughput screening	(69)
5	Airan et. al.	2012	PKA sensor	(1) Synthetic gene that with heterogeneous amino acid sequence (2) effect of phosphorylation on the contrast	(72)
6	Bar-Shir et. al.	2014	Human protamine as a reporter gene	DNA optimization improves contrast	(75)
7	Oskolkov et. al.	2014	Characterization of Human Protamine	(1) Effect of phosphorylation and (2) effect of intermolecular bonds on the contrast	(76)
8	Bar-Shir et. al.	2015	Supercharged GFP as a CEST based reporter	The contrast can be improved by changing only limited number of amino acids	(74)